



Reduced quantum confinement effect and electron-hole separation in SiGe nanowires

Michele Amato,¹ Maurizia Palummo,² and Stefano Ossicini^{3,*}

¹Dipartimento di Fisica and CNR-INFM-S³ “NanoStructures and BioSystems at Surfaces,”
Università di Modena e Reggio Emilia, via Campi 213/A, 41100 Modena, Italy

²Dipartimento di Fisica, European Theoretical Spectroscopy Facility (ETSF), CNR-INFM-SMC,
Università di Roma, “Tor Vergata,” via della Ricerca Scientifica 1, 00133 Roma, Italy

³Dipartimento di Scienze e Metodi dell’Ingegneria and CNR-INFM-S³ “NanoStructures and BioSystems at Surfaces,”
Università di Modena e Reggio Emilia, via Amendola 2 Padiglione Morselli, I-42100 Reggio Emilia, Italy

(Received 9 April 2009; published 11 May 2009)

Using first-principles methods, we investigate the structural and electronic properties of SiGe nanowires-based heterostructures, whose lattice contains the same number of Si and Ge atoms but arranged in a different manner. Our results demonstrate that the wires with a clear interface between Si and Ge regions not only form the most stable structures but show a strongly reduced quantum confinement effect. Moreover, we, with the inclusion of many-body effects, prove that these nanowires—under optical excitation—display a clear electron-hole separation property which can have relevant technological applications.

DOI: [10.1103/PhysRevB.79.201302](https://doi.org/10.1103/PhysRevB.79.201302)

PACS number(s): 73.22.-f, 73.20.At, 78.67.Bf

The possibility to tailor the properties of semiconductor nanostructures render them interesting for several important technological fields. A variety of applications, using nanowires (NWs) as sensors,¹ electronic,² photonic,^{3,4} nanomechanical,⁵ nanoprocessors,⁶ and thermoelectric⁷ devices, has been demonstrated. Many experimental^{8–14} and theoretical^{15–26} studies have been carried out to investigate the structural and optoelectronic properties of Si, Ge, and SiGe NWs. It has been demonstrated that the quantum confinement effect (QCE) leads to an increase in the band gap with decreasing wire diameter and, thus, to a blueshift of the absorption and emission spectra. For SiGe NWs, particular attention has been devoted to the core/shell NWs, where a further possibility of tuning the band gap has been envisaged by varying the composition of the heterostructures and the geometry of interface between the two materials.^{20,23} Moreover the core/shell NWs exhibited important performance as high-mobility FET’s (Ref. 12) and low-temperature quantum devices^{13,14} showing their immense potential for fabrication of a new generation of nanodevices, compatible with the actual Si technology. Here we consider different types of SiGe NWs, and we prove that the NWs, which exhibit a clear interface between Si and Ge region, form the most stable structures and show a strongly reduced QCE with respect to the other ones. Indeed we demonstrate that in these NWs, there is a clear spatial separation between Ge-related valence states and Si-related conduction states. Moreover, the spatial distribution of the lowest exciton obtained by the solution of the Bethe-Salpeter equation (BSE) points out the electron-hole (e-h) separation under optical excitation. We think that this interesting property to quantum confine holes and electrons in different region of the NW can become suitable for developing new nanodevices such as Si-based solar cells.

The free-standing NWs considered here have an approximately cylindrical shape and are oriented along the [110] direction (the preferred growth direction at small diameters¹⁰) and with diameter ranging from 0.8 to 1.6 nm.²⁷ The process of constructing the input geometry of the NWs is the same in Refs. 17 and 21. The surface dangling bonds are saturated with H atoms to remove the corresponding lo-

calized surface states from the fundamental energy-band-gap range. Pure Si NWs and Ge NWs and SiGe heterostructures (SiGe NWs) with fixed composition Si=0.5 and Ge=0.5 have been studied.²⁸

The top views of the pure NWs are shown in Figs. 1(a) and 1(b). For the mixed SiGe NWs, we distinguish three different types of structures, with the same composition, the same geometry, but different distribution of the two types of atoms (called *homotops*²⁹). The first one is random SiGe NWs (*random* NWs), where the distribution of the two type of atoms in the lattice unit cell is completely random [see Fig. 1(c)]; the second one is mixed SiGe NWs (*mixed* NWs), in which a type of atom is bonded in a tetrahedral geometry with four atoms of the other type [see Fig. 1(d)]; and the last one is half SiGe NWs (*half* NWs), where one half of cross section of the NW is made up of Si and the other half is made up of Ge atoms [see Fig. 1(e)].

We performed *ab initio* calculations within the single-particle density functional theory in the local-density approximation (DFT-LDA), as implemented in the QUANTUM-ESPRESSO package.^{30,31} In order to explicitly calculate the e-h wave function and the distribution probability in real space of the lowest exciton (for one of the half NWs), we have

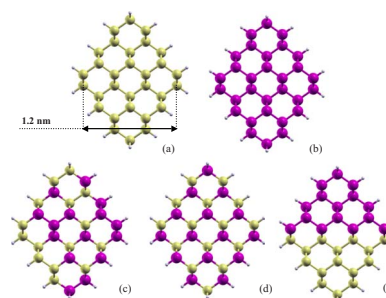


FIG. 1. (Color online) Top view of (a) Si, (b) Ge, and (c) SiGe random, (d) mixed, and (e) half nanowires with a diameter $d=1.2$ nm. Yellow/light gray spheres represent Si atoms and magenta/dark gray spheres represent Ge atoms, while the small white spheres are H atoms used to saturate the dangling bonds.

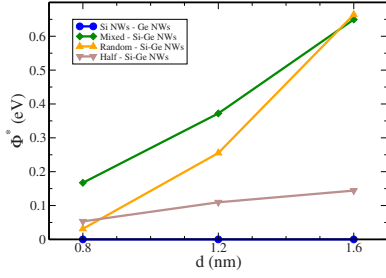


FIG. 2. (Color online) Formation enthalpy for random, mixed, and half SiGe NWs as function of their diameter. The same quantity for the corresponding pure Si or Ge NWs is also shown (the two curves here coincide, being both zero at any diameter).

performed, on top of the one-particle calculation, a many-body calculation of the charged and neutral excitations by means of the self-energy (GW) and BSE approaches.^{32,33} In the Green's functions formalism, the solution of the BSE corresponds to diagonalizing the following excitonic problem:

$$(\epsilon_{ck} - \epsilon_{vk})A_{cvk}^\lambda + \sum_{c'v'k'} \langle cvk|W - 2V|c'v'k'\rangle A_{c'v'k'}^\lambda = E_\lambda A_{cvk}^\lambda, \quad (1)$$

where $(\epsilon_{ck} - \epsilon_{vk})$ are the quasiparticle energies obtained within a GW calculation, W is the statically screened, V is the bare Coulomb interaction, and A_{cvk}^λ are the excitonic amplitudes. In this way the e-h wave function, corresponding to the exciton energy E_λ , is obtained as

$$\psi^\lambda(r_e, r_h) = \sum_{c,v,k} A_{cvk}^\lambda \psi_{c,k}(r_e) \psi_{v,k}^*(r_h). \quad (2)$$

As first step, to have the information about the thermodynamic stability of the NWs of interest, we have calculated their formation enthalpy (FE) and we have investigated its dependence on the atomic configuration in the unit cell and on the wire's diameter. This quantity useful for the synthesis of the NWs has been calculated assuming zero pressure and neglecting the vibrational contribution and the zero-point energy. To have a realistic description of the FE, which can be comparable with the experiment, we have evaluated it in the way proposed in Ref. 34,

$$\Phi^*(\text{Si}_n\text{Ge}_m\text{H}_l) = E_{\text{tot}}(\text{Si}_n\text{Ge}_m\text{H}_l) - m \cdot \frac{E_{\text{tot}}(\text{Ge}_N\text{H}_l)}{N} - n \cdot \frac{E_{\text{tot}}(\text{Si}_N\text{H}_l)}{N}, \quad (3)$$

where E_{tot} is the ground-state total energy of a given $\text{Si}_n\text{Ge}_m\text{H}_l$ NW and $N=n+m$. In Eq. (3) we are subtracting from the E_{tot} of the nanoalloy the appropriate fraction of the configurational energy of the pure reference Si and Ge NWs. The results are shown in Fig. 2.

The most stable structure is characterized by the lowest value of Φ^* . Observing the data, it is clear that at any diameter, the most stable SiGe NWs are the half NWs. Increasing the diameter, we note that the absolute value of the difference between the FE of different SiGe NWs increases. In particular, it is possible to say that at large diameter, the SiGe

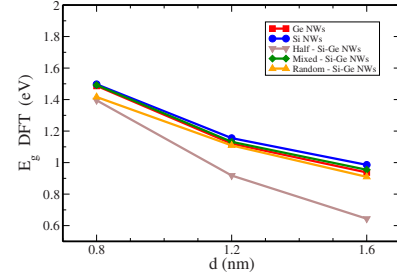


FIG. 3. (Color online) DFT-LDA electronic gaps as a function of NW diameter for random, mixed, and half NWs: a fixed composition. The corresponding gaps of pure Si and Ge NWs are also shown.

systems tend to segregate and not mix. In fact, at small diameter, the difference of Φ^* between mixed NWs and half NWs is small (≈ 0.10 eV), while, increasing the diameter, this difference becomes larger (≈ 0.5 eV). The behavior of random NWs at small diameter is close to half NWs (at 0.8 nm the two values of Φ^* practically coincide), this is due to the fact that when the diameter is small the number of possible configurations is low and so a random structure will be more *segregated* (i.e., more close to a half NW) rather than *mixed* (where there is not any form of segregation). On the contrary, at large diameter, the behavior of random NWs is similar to that of mixed NWs; now the number of possible configurations for a random NW is larger, the probability for these NWs to be segregated is lower and the FE increases. In conclusion, the segregation results in a gain in energy and for larger diameter it is clearly favored with respect to any form of mixing.

We aim to move now to the discussion of the electronic properties of these NWs. Several theoretical studies have demonstrated that the energy-band gap (E_G) of [110] Si and Ge NWs decreases monotonically with the wire's diameter,^{17,18,21,26} as a clear consequence of the QCE. Other studies on SiGe core-shell NWs have shown a strong linear composition dependence of E_G .^{20,35} In the following we report in Fig. 3, the trend of the electronic DFT-LDA E_G as a function of the wire's diameter for mixed, random, half NWs, comparing it with the corresponding trend in pure Si and Ge NWs.

The trend for pure NWs is in very good agreement with other studies.^{17,18} The most interesting result, here, is that the half NWs show a strongly reduced QCE (RQCE), which appears to be more pronounced increasing the diameter of the wire. This property is absent in mixed and random NWs, which have E_G very close to those obtained for pure Si and Ge NWs, even if they have the same composition of the half NWs ($x_{\text{Si}}=0.5$ and $x_{\text{Ge}}=0.5$). Thus it can be envisaged that this effect must be related to the geometry of the NW, in particular, to the configuration of the atoms in the unit cell and to the presence of a clear interface between Si and Ge regions. In particular, as we will show later on, its physical origin is due to the type II band offset which comes out at the interface between Si and Ge atoms³⁶ and is related to a consequent spatial carrier localization (SCL). Since the contribution to the QCE for Si and Ge is very different, this creates a different alignment of the conduction and valence states

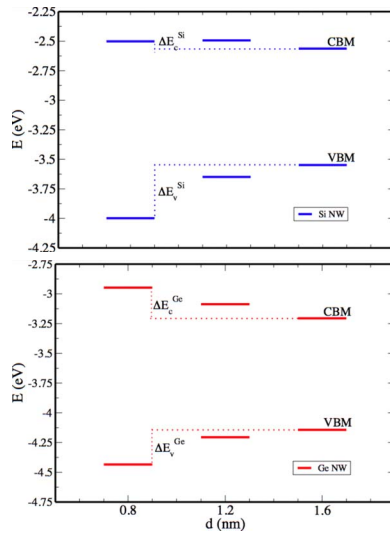


FIG. 4. (Color online) Variation in the VBM and CBM energies as a function of the diameter for pure Si (top) and pure Ge (bottom) NWs.

and as consequence a reduced E_G compared to pure NWs of the same diameter.

In order to quantitatively demonstrate this point, we reported in Fig. 4 the position in energy relatively to the vacuum level (taken as zero) of the valence-band maximum (VBM) and the conduction-band minimum (CBM) (both at Γ point since all NWs have a direct band gap) of pure Si and Ge NWs. The vacuum level is calculated from the cylindrical average local potential in the vacuum region, where it becomes a constant in the supercell.

In Fig. 4 we show also the energy variation in the VBM ΔE_v and of the CBM ΔE_c , with respect to their values in the largest NWs.³⁷ We note that ΔE_v^{Si} is larger than ΔE_v^{Ge} , while ΔE_c^{Si} is smaller than ΔE_c^{Ge} . Moreover, it comes out that the ratio $\frac{\Delta E_v}{\Delta E_c}$ is nearly 1 for Ge NWs, while it is nearly 2 for Si NWs. Other studies, in zero- and one-dimensional nanostructures^{18,38} proposed a similar quantitative analysis, evaluating the shift from the bulk values of the conduction- and valence-band edge due to the QCE. They found that the E_G opens with a fixed ratio of the valence to the conduction-band-edge shift equal to ~ 2 for Si and to ~ 1 for Ge nanostructures. Furthermore, the obtained trends of the VBM and CBM energies are consistent with the experimental results obtained for zero-dimensional nanostructures by Bostedt *et al.*³⁹ and van Buuren *et al.*⁴⁰ who found that the QCE on Ge nanocrystals is always stronger than in Si nanocrystals. Regarding the NWs, the results reported in Fig. 4 can give a strong indication about the origin of Si/Ge band offset in the half NWs and consequently the RQCE. When the QCE opens the E_G of the bulk material, we can note different behaviors for the valence and conduction bands. The VBM tends to be more shifted down for the Si than for the Ge ($\Delta E_v^{\text{Si}} > \Delta E_v^{\text{Ge}}$), so finally the edge of the valence band is localized on the Ge region of the wire; whereas in the case of the CBM an opposite behavior is observed, the shift is more pronounced for Ge than for Si ($\Delta E_c^{\text{Ge}} > \Delta E_c^{\text{Si}}$), thus the edge of the wire's conduction band is localized on the Si region.

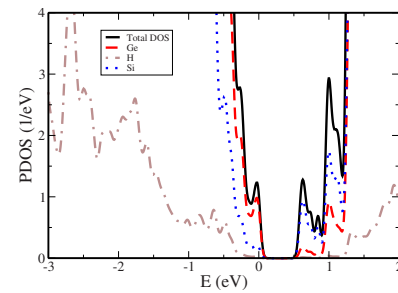


FIG. 5. (Color online) Total density of states (black-solid line) and PDOS on the different atoms in the NW for half NW ($d=1.6$ nm). Ge atoms (red-dashed line), Si atoms (blue-dotted line), and H atoms (brown-dot-dashed line).

The calculated projected density of states (PDOS) reported in Fig. 5 for the half NWs with a diameter of 1.6 nm is a clear confirmation of this analysis. The projection is done onto the atomic orbitals of each atom in the NWs.

The PDOS shows, clearly, that the contribution to the total DOS (black-solid line) of the NW is principally due to Ge atoms (red-dashed line) for the valence and to Si atoms (blue-dotted line) for the conduction states. To understand this point deeper, we have carefully analyzed the spatial localization of the electronic wave functions of the VBM and CBM, in all the SiGe NWs with a diameter of 1.6 nm reported in Fig. 6.

Three important conclusions can be drawn from Fig. 6: (i) the half NWs show a clear localization of the conduction states on Si atoms and of the valence states on Ge atoms; we found that this property is more pronounced by increasing the diameter (such as the behavior of the E_G), (ii) the shape and the localization of the VBM and CBM wave functions for mixed NWs are very similar to that of the pure NWs and do not present any hint of a spatial localization of the states on a specific material, and (iii) in random NWs, one can recognize some regions, where a partial spatial localization of the electronic states—near Si or Ge atoms—is present. Also here the VBM is preferentially localized on Ge islands, while the CBM on Si islands. Then, the SCL is strictly related to the NW geometry: in particular, it depends on the dimension of the interface between Si and Ge regions. In fact

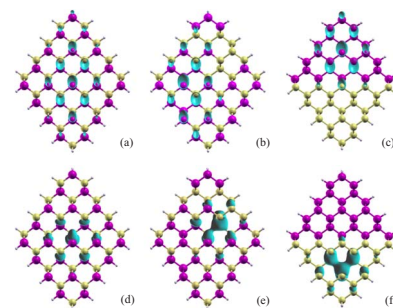


FIG. 6. (Color online) VBM (top) and CBM (bottom) wave function localizations for [(a) and (d)] mixed, [(b) and (e)] random, and [(c) and (f)] half SiGe NWs with diameter $d=1.6$ nm. Yellow/light gray spheres represent Si atoms and magenta/dark gray spheres represent Ge atoms, while the small white spheres are H atoms used to saturate the dangling bonds.

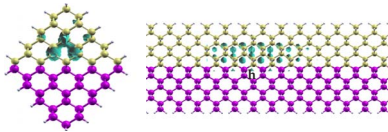


FIG. 7. (Color online) Top (left panel) and side (right panel) views of the electron distribution probability; the hole position is fixed on top of the central Ge atom. Yellow/light gray spheres represent Si atoms and magenta/dark gray spheres represent Ge atoms, while the small white spheres are H atoms used to saturate the dangling bonds. The isosurface of the e-h distribution probability is shown in celestial.

this effect is very pronounced on half NWs that exhibit a large Si/Ge interface in the transverse section of the wire; it is present in random NWs, which show some small interfaces between Si and Ge islands and it is completely absent in mixed NWs, where there is not any Si/Ge interface.

The present analysis is strongly confirmed by the many-

body localization of the lowest exciton of the half NW with $d=1.6$ nm, as obtained by the solution of the BSE and shown in Fig. 7. Fixing the hole position on top of the central Ge atom near the Si/Ge interface, the electron distribution probability is clearly localized on the Si-atoms region, confirming a straightforward tendency to an e-h separation in these types of NWs.

From the bottom panel of Fig. 7, an exciton localization, along the wire axis, of about 25 Å can be estimated. The strong e-h pair separation can play an important role in solar cell devices.^{41,42} Moreover, by suitable doping in different regions, one can envisage important technological applications of these SiGe NWs, as advanced thermoelectric materials^{7,43} and in quantum computing.⁴⁴

We acknowledge MIUR-PRIN 2007, CINECA-CNR-INFN (for CPU time), and Ec e-I3 ETSF project (INFRA: No. 211956).

*stefano.ossicini@unimore.it

- ¹Y. Cui and C. M. Lieber, *Science* **291**, 851 (2001).
- ²Y. Huang *et al.*, *Science* **294**, 1313 (2001).
- ³O. Hayden *et al.*, *Nature Mater.* **5**, 352 (2006).
- ⁴C. J. Barrelet *et al.*, *Nano Lett.* **6**, 11 (2006).
- ⁵N. A. Melosh *et al.*, *Science* **300**, 112 (2003).
- ⁶Y. Dong *et al.*, *Nano Lett.* **8**, 386 (2008).
- ⁷A. I. Hochbaum *et al.*, *Nature (London)* **451**, 163 (2008).
- ⁸L. Lauhon *et al.*, *Nature (London)* **420**, 57 (2002).
- ⁹D. D. D. Ma *et al.*, *Science* **299**, 1874 (2003).
- ¹⁰Y. Wu *et al.*, *Nano Lett.* **4**, 433 (2004).
- ¹¹J. Yang *et al.*, *Nano Lett.* **6**, 2679 (2006).
- ¹²J. Xiang *et al.*, *Nature (London)* **441**, 489 (2006).
- ¹³J. Xiang *et al.*, *Nat. Nanotechnol.* **1**, 208 (2006).
- ¹⁴Y. Hu *et al.*, *Nat. Nanotechnol.* **2**, 622 (2007).
- ¹⁵A. Nduwimana *et al.*, *Nano Lett.* **8**, 3341 (2008), and references therein.
- ¹⁶A. N. Kholod *et al.*, *Phys. Rev. B* **70**, 035317 (2004).
- ¹⁷M. Bruno *et al.*, *Phys. Rev. B* **72**, 153310 (2005).
- ¹⁸S. P. Beckman, J. Han, and J. R. Chelikowsky, *Phys. Rev. B* **74**, 165314 (2006).
- ¹⁹R. Kagimura, R. W. Nunes, and H. Chacham, *Phys. Rev. Lett.* **98**, 026801 (2007).
- ²⁰R. N. Musin and X. Q. Wang, *Phys. Rev. B* **74**, 165308 (2006).
- ²¹M. Bruno *et al.*, *Phys. Rev. Lett.* **98**, 036807 (2007).
- ²²N. Akman *et al.*, *Phys. Rev. B* **76**, 245427 (2007).
- ²³D. B. Migas and V. E. Borisenko, *Phys. Rev. B* **76**, 035440 (2007).
- ²⁴Y. Zhang and Y. Xiao, *Eur. Phys. J. B* **63**, 425 (2008).
- ²⁵K. Hong *et al.*, *Nano Lett.* **8**, 1335 (2008).
- ²⁶D. Yao *et al.*, *Nano Lett.* **8**, 4557 (2008).
- ²⁷A. Filonov *et al.*, *Appl. Phys. Lett.* **67**, 1090 (1995).
- ²⁸The optimized bulk lattice parameter used to calculate the translational periodicity, along the wire axis, is $a_{\text{Si}}=5.40$ Å for pure Si NWs, $a_{\text{Ge}}=5.59$ Å for pure Ge NWs, and $a_{\text{Si/Ge}}=5.49$ Å for SiGe NWs; in this last case we follow the Vegard's law for alloys. The input Ge-H bond length (0.1525 nm) and the input Si-H bond length (0.1480 nm) correspond to that of the GeH₄ molecule and of SiH₄ molecule, respectively. It is important to point out that for SiGe NWs, we have carefully checked the effect of different lattice parameters (pure Si, pure Ge, and Vegard's law) on the electronic properties finding that they are really independent from the choice of the lattice constant.
- ²⁹J. Jellinek and E. Krissinel, *Chem. Phys. Lett.* **258**, 283 (1996).
- ³⁰S. Baroni *et al.*, <http://www.pwscf.org/>
- ³¹Norm-conserving pseudopotentials have been used. The supercell is taken to be large enough (more than 10 Å of vacuum) orthogonal to the growth direction to eliminate the interaction between neighbor wires. The NWs geometries have been relaxed with direct energy minimization technique in the way that the forces on each atom are less than 0.003 Ry/a.u. An energy cutoff to 30 Ry and a grid of $16 \times 1 \times 1$ points for the sampling of the Brillouin zone have been used.
- ³²G. Onida, L. Reining, and A. Rubio, *Rev. Mod. Phys.* **74**, 601 (2002).
- ³³A. Marini *et al.*, *Comput. Phys. Commun.* (to be published).
- ³⁴R. Ferrando, J. Jellinek, and R. L. Johnston, *Chem. Rev. (Washington, D.C.)* **108**, 845 (2008).
- ³⁵For core-shell SiGe NWs we found, as in Ref. 20, that the band-gap opening strongly depends on the material localization (core vs shell) and composition.
- ³⁶C. Van de Walle and R. Martin, *J. Vac. Sci. Technol. B* **3**, 1256 (1985).
- ³⁷The calculated ratio is referred to the VBM and CBM shifts with respect to their values for the NW with 1.6 nm. This is not a strong approximation because we are interested only in how the confinement behavior of the material scales with the diameter, and so we can assume the largest wire as our reference.
- ³⁸F. A. Reboredo *et al.*, *Phys. Rev. B* **61**, 13073 (2000).
- ³⁹C. Bostedt *et al.*, *Appl. Phys. Lett.* **84**, 4056 (2004).
- ⁴⁰T. van Buuren *et al.*, *Phys. Rev. Lett.* **80**, 3803 (1998).
- ⁴¹G. Conibeer *et al.*, *Thin Solid Films* **511-512**, 654 (2006).
- ⁴²S. Lu and A. Madhukar, *Nano Lett.* **7**, 3443 (2007).
- ⁴³M. N. Tripathi and C. M. Bhandari, *Eur. Phys. J. B* **59**, 503 (2007).
- ⁴⁴R. Vrijen *et al.*, *Phys. Rev. A* **62**, 012306 (2000).